International Journal of Power Electronics and Drive Systems (IJPEDS)
Vol. 12, No. 3, September 2021, pp. 1358~1368
ISSN: 2088-8694, DOI: 10.11591/ijpeds.v12.i3.pp1358-1368

Real time implementation of anti-windup PI controller for speed control of induction machine based on DTC strategy

Lahcen Ouboubker[1], Jawad Lamterkati[2], Mohamed Khafallah[3], Aziz El Afia[4]
[1]Faculty of Applied Sciences of Ait Melloul, Ibn Zohr University, Agadir, Morocco
[1]LGEMS Laboratory, National School of Applied Sciences of Agadir, Ibn Zohr University, Agadir, Morocco
[2]RITM Laboratory, High School of Technology, Hassan II University, Casablanca, Morocco
[1,2,3,4]Energy and Electrical Systems Laboratory, ENSEM, Hassan II University, Casablanca, Morocco
[4]ENSAM, Hassan II University, Casablanca, Morocco

Article Info

Article history:

Received Dec 29, 2020
Revised Jun 2, 2021
Accepted Jul 13, 2021

Keywords:

Anti-windup PI controller
Direct torque control
dSPACE 1104
Induction machine
Real time implementation
Speed drive

ABSTRACT

This paper presents simulation and experimental results of anti-windup PI controller to improve induction machine speed control based on direct torque control (DTC) strategy. Problems like rollover can arise in conventional PI controller due to saturation effect. In order to avoid such problems anti-windup PI controller is presented. This controller is simple for implementation in practice. The proposed anti-windup PI controller demonstrates better dynamic step changes response in speed in terms of overshoots. All simulation work was done using Simulink in the MATLAB software. The experimental results were obtained by practical implementation on a dSPACE 1104 board for a 1.5 KW induction machine. Simulation and experimental results have proven a good performance and verified the validity of the presented control strategy.

Corresponding Author:

Lahcen Ouboubker
Departement of Physics
Faculty of Applied Sciences of Ait Melloul
LGEMS, ENSA, Ibn Zohr University, Agadir BP 1136, Morocco
Email: l.ouboubker@uiz.ac.ma

1. INTRODUCTION

Traditionally, DC motors are used for speed variation of electric machines, because the magnetic flux and electromagnetic torque are easily controlled by the stator and rotor current, respectively [1]. In the last two decades, AC motors are replacing DC motors. The induction machine (IM) is the most robust and responsive AC motor in the industry. However, its nonlinear and highly coupled structure presents a limitation to the performance of the control of this induction machine [2]. In the last decade, a new control method called DTC has been introduced. DTC has received considerable attention in industrial motor drive applications. The main reason for its popularity is due to its simple structure, robustness to rotor parameter variations and fast dynamic response [3].

Direct torque control (DTC) has been developed to replace traditional PWM drives of the open- and closed-loop type used in FOC [4]. DTC has several advantages: torque response, torque repeatability, motor dynamic and static speed accuracy [5]. The DTC method is characterized by a switching table that determines the voltage vector to be applied for controlling the switches of the voltage inverter [6]. This control method is very simple. It allows decoupled control to flux and torque without resorting to use the technique of width modulation and pulse current regulators [6]. This type of control is based on non-linear correctors of the hysteresis type which present limitations in case of large switching and uncontrollable frequency [6].

On the other hand, the design of the speed controller greatly affects the performance of the drive. Vector control generally uses proportional-integral (PI) speed controller as inner speed loop to generate torque current [7], [8]. PI speed controller is often used because it can reduce steady state error and easy to implement. To get fast dynamic response, high PI gains cause undesirable system behavior such as high overshoot and slow settling time. On the other hand, integral-proportional (IP) speed controller has been presented in [8], [9], [10] that provide better performance in reducing or eliminating overshoot, but still gives fast dynamic response.

Both speed controller schemes on conventional PI and conventional IP are designed without considering the limit of controller output. Whereas, in real condition, a control system will find the saturation problem. When it saturated, the feedback loop can be damaged and the system works like an open loop system. In addition, the existence of integral action that responds to accumulated errors from the past can lead to large overshoot, delayed response, slow settling time, even system instability. This problem is called windup effect. Anti-windup strategies are available in order to solve the problem of windup effect [11], [12].

The conventional antiwindup methods include: (i) conditional integration [13]-[15], where the integral action is activated or deactivated depending on certain conditions, the integration being suspended in case of saturation and the control error is of the same sign as the control signal; (ii) the use of a limited integrator [16], where the integrator value is limited to the linear range of the actuator by hard feedback via a high-gain dead zone; (iii) in [17]-[19] a classical method for computing feedback in which the difference between the saturated and unsaturated control signal is used to generate a feedback signal that acts on the integrator input is presented [20]. Unified anti-doubling strategies that combine the tracking back calculation and conditional integration approaches are presented in [20], [21].

In this work we present an anti-windup PI speed control for an induction machine based on a direct torque control strategy, in order to eliminate the undesirable side effect known as integrator windup. The proposed anti-windup controller has some advantages: almost zero overshoot and very simple implementation in existing PI controllers. To validate our approach, the Anti-windup PI controller performances for induction machine speed control based on direct torque control strategy have been investigated by simulations under MATLAB/Simulink and the validity of the proposed control scheme is proved by the experimental results on dSPACE system with DS1104 controller board.

2. INDUCTION MACHINE AND THREE PHASE INVERTER MODELING

Figure 1 shows a simplified circuit diagram of a conventional two-level voltage inverter feeding an induction machine. The delivered voltage vector depends on the state of the switches S_a, S_b, S_c and the DC voltage E.

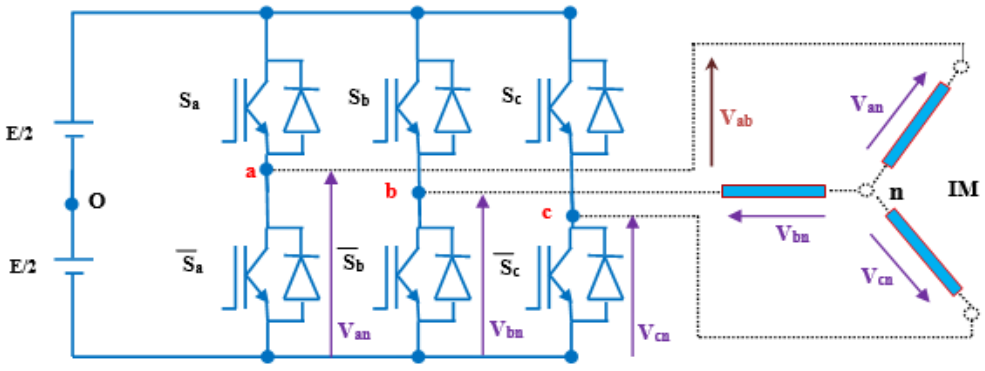

Figure 1. Three-phase voltage inverter fed induction machine

2.1. Modeling of the three-phase inverter

The function of the inverter is to convert the direct voltage into alternating one. The DC-AC converter is composed of 6 insulated gate bipolar transistors (IGBTs) to control the three-phase induction machine. The aim of this kind of system is to manage the amplitude and frequency of the stator voltages. The three-phase inverter model contains eight switching states. Figure 2 shows the representation of each IGBT state based on a vector presentation.

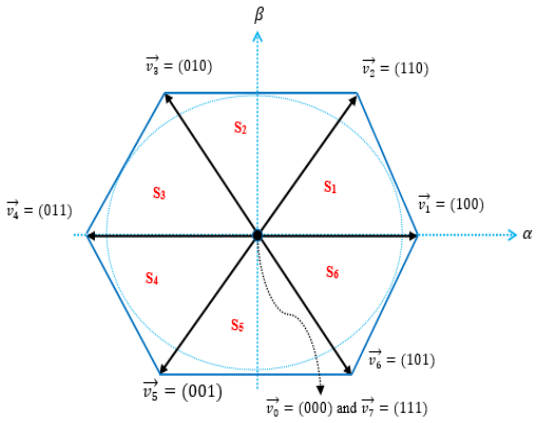

Figure 2. Operating conditions of three-phase inverter: vector presentation of the voltages

The stator phase voltages are described in (1) using literature [22], where V(a,b,c) are the three phase stator voltages, E is the DC link voltage and S(a,b,c) are the switching functions that can take two logic values 0 or 1.

$$\begin{cases} v_{an} = \frac{E}{3}(2S_a - S_b - S_c) \\ v_{bn} = \frac{E}{3}(-S_a + 2S_b - S_c) \\ v_{cn} = \frac{E}{3}(-S_a - S_b + 2S_{c)} \end{cases} \quad (1)$$

The output voltage of the inverter is defined in (2) and (3) using the vector presentation.

$$v_s = v_{s\alpha} + jv_{s\beta} \quad (2)$$

$$\begin{bmatrix} v_{s\alpha} \\ v_{s\beta} \end{bmatrix} = \begin{bmatrix} 1 & -\frac{1}{2} & -\frac{1}{2} \\ 0 & \frac{\sqrt{3}}{2} & -\frac{\sqrt{3}}{2} \end{bmatrix} \begin{bmatrix} v_{an} \\ v_{bn} \\ v_{cn} \end{bmatrix} \quad (3)$$

Then, v_s can be expressed using (4). The (4) allows the determination of the voltage for each sector using the vector presentation.

$$v_s = \sqrt{\frac{2}{3}} E(S_a + e^{j\frac{2\pi}{3}} S_b + e^{j\frac{4\pi}{3}} S_c) \quad (4)$$

2.2. Modeling of the three-phase induction machine

The induction machine is a nonlinear and unsymmetrical system. As reported in literature, the stator and rotor voltage equations can be represented in a stationary reference frame using (5) and (6) [23]-[25]. The (7) and (8) give the stator flux equations. The parameters of these equations are defined by:

$v_{s\alpha}$, $v_{s\beta}$: α-β stator voltages
$i_{s\alpha}$, $i_{s\beta}$, $i_{r\alpha}$, $i_{r\beta}$: stator and rotor currents;
$\phi_{s\alpha}$, $\phi_{s\beta}$, $\phi_{r\alpha}$, $\phi_{r\beta}$: α-β stator and rotor flux;
R_s, R_r : stator and rotor resistances;
Ls, Lr : stator and rotor inductances;
M : mutual inductance;
np : machine pole pairs.

$$\begin{bmatrix} v_{s\alpha} \\ v_{s\beta} \end{bmatrix} = R_s \begin{bmatrix} i_{s\alpha} \\ i_{s\beta} \end{bmatrix} + \frac{d}{dt} \begin{bmatrix} \phi_{s\alpha} \\ \phi_{s\beta} \end{bmatrix} \quad (5)$$

$$\begin{bmatrix} v_{r\alpha} \\ v_{r\beta} \end{bmatrix} = \begin{bmatrix} 0 \\ 0 \end{bmatrix} = R_r \begin{bmatrix} i_{r\alpha} \\ i_{r\beta} \end{bmatrix} + \frac{d}{dt} \begin{bmatrix} \phi_{r\alpha} \\ \phi_{r\beta} \end{bmatrix} + \omega[G] \begin{bmatrix} \phi_{r\alpha} \\ \phi_{r\beta} \end{bmatrix} \quad (6)$$

$$\begin{bmatrix} \phi_{s\alpha} \\ \phi_{s\beta} \end{bmatrix} = [L_s] \begin{bmatrix} i_{s\alpha} \\ i_{s\beta} \end{bmatrix} + [M] \begin{bmatrix} i_{r\alpha} \\ i_{r\beta} \end{bmatrix} \quad (7)$$

$$\begin{bmatrix} \phi_{r\alpha} \\ \phi_{r\beta} \end{bmatrix} = [L_s] \begin{bmatrix} i_{r\alpha} \\ i_{r\beta} \end{bmatrix} + [M] \begin{bmatrix} i_{s\alpha} \\ i_{s\beta} \end{bmatrix} \quad (8)$$

3. BASIC DTC OF INDUCTION MACHINE DRIVE

DTC is a vector control method used to control the torque and therefore the speed of the induction machine by controlling the switching sequence of the inverter transistors. The Figure 3 shows the basic DTC principle. The DTC provides direct and independent the control of the flux and torque of an induction machine by selecting the optimal switching modes of the voltage inverter. it allows the flux and torque to be maintained within their hysteresis bands. Thus, DTC provides very fast torque response without using coordinate transformation, current controllers and PWM generator. In the DTC, the machine torque control is achieved with two hysteresis controllers, one for stator flux magnitude error and the other for the torque magnitude error. The selection of one switching vector per sampling time depends on the sign of these two controllers [6].

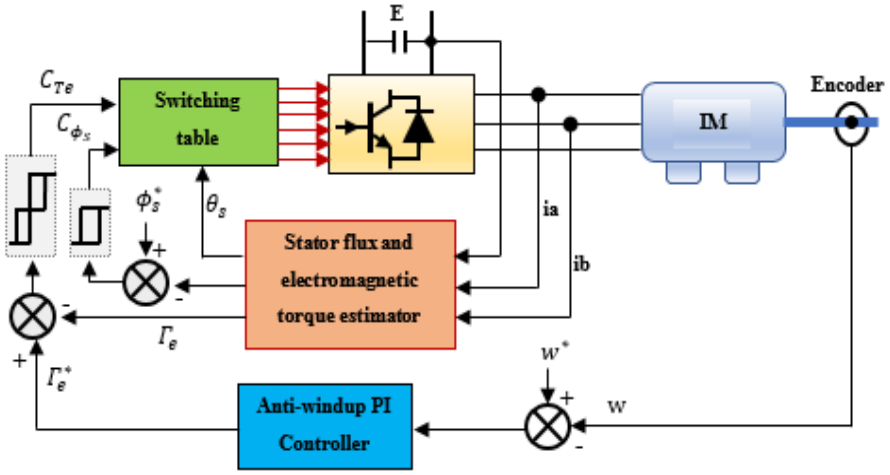

Figure 3. Basic DTC scheme for induction machine drive with speed loop

By using a (α, β) stationary stator reference frame, the stator flux linkage ϕ_s and electromagnetic torque Γ_e are calculating by using (9) and (10):

$$\phi_{s\alpha} = \int_0^t (V_{s\alpha} - R_s I_{s\alpha}) dt \quad (9)$$

$$\phi_{s\beta} = \int_0^t (V_{s\beta} - R_s I_{s\beta}) dt \quad (10)$$

The stator flux linkage phasor is given by (11):

$$\phi s = \sqrt{\phi_{s\alpha}^2 + \phi_{s\beta}^2} \quad (11)$$

The angle θ_s is equal to:

$$\theta_s = tan^{-1}\left(\frac{\phi_{s\beta}}{\phi_{s\alpha}}\right) \quad (12)$$

The estimated electromagnetic torque is given by (13):

$$T_e = np\left[\phi_{s\alpha} I_{s\beta} - \phi_{s\beta} I_{s\alpha}\right] \quad (13)$$

The error between the estimated torque Γ_e and the reference torque Γ_e^* is the input of a three level hysteresis comparator, whereas the error between the estimated stator flux magnitude ϕ_s and his reference stator flux magnitude ϕ_s^* is the input of a two level hysteresis comparator. Figure 4 (a) and Figure 4 (b) illustrate the flux and torque comparators.

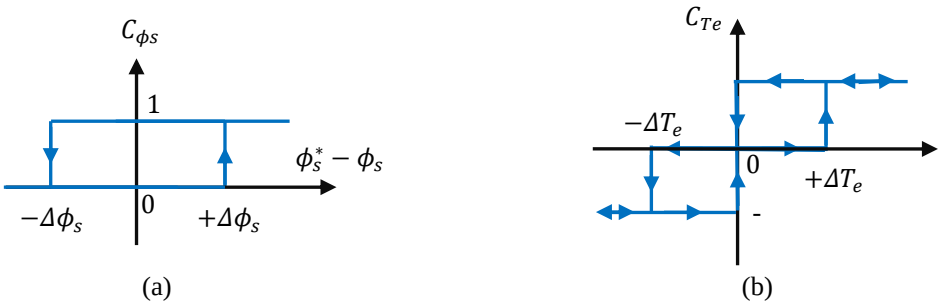

Figure 4. Hysteresis comparators, (a) flux hysteresis comparator; (b) torque hysteresis comparator

To determine the stator voltage vector to be applied, the circular stator flux path is first divided into six symmetrical sectors (Figure 5) [6]. Then, the effect of each stator vector voltage on the flux and torque is studied. The selection of the adequate voltage vector is based on the switching table given in Table 1. The inputs quantities are the flux sector and the outputs of the two hysteresis comparators.

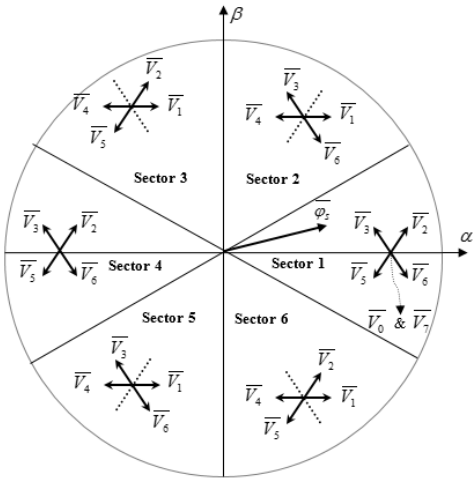

Figure 5. Influence of the voltage vector selected on the variation of stator flux modulus and torque

Table 1. Switching table

$C_{\phi s}$	Sector Si / C_{Te}	S_1	S_2	S_3	S_4	S_5	S_6
1	1	V_2	V_3	V_4	V_5	V_6	V_1
	0	V_7	V_0	V_7	V_0	V_7	V_0
	-1	V_6	V_1	V_2	V_3	V_4	V_5
0	1	V_3	V_4	V_5	V_6	V_1	V_2
	0	V_0	V_7	V_0	V_7	V_0	V_7
	-1	V_5	V_6	V_1	V_2	V_3	V_4

V_0=[0,0,0] ; V_1=[1,0,0] ; V_2=[1,1,0] ; V_3=[0,1,0] ; V_4=[0,1,1] ; V_5=[0,0,1] ; V_6=[1,0,1] ; V_7=[1,1,1]

4. ANTI-WINDUP PI CONTROLLER

The structure of the anti-windup PI controller based on the back-calculation method is presented in Figure 6. The saturation error u_e and anti-windup gain K are the main parameters for the integral action correction, where:

$$ue = uin - uout \tag{14}$$

A feedback signal is generated from the difference between the saturated and unsaturated control signals and is used to reduce the integrator input when the controller output exceeds the actuator limits. The saturation in Figure 6 can either be a model used in the controller or the actual saturation of the actuator if its output is measurable.

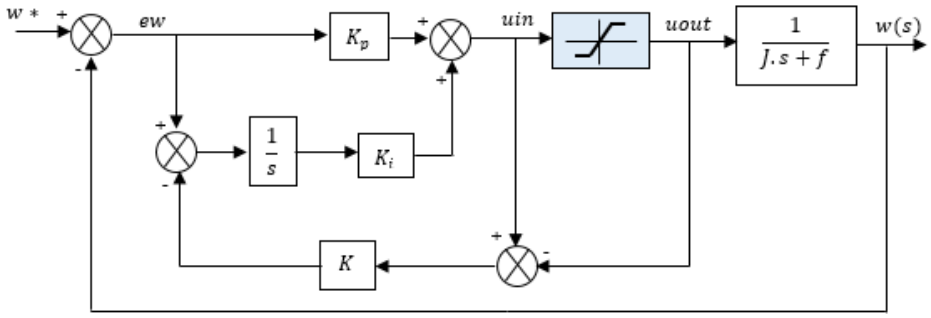

Figure 6. Anti-windup PI controller based on back calculation method

5. SIMULATION RESULTS AND DISCUSSION

In order to evaluate the performance of the proposed control strategy, simulation tests were carried out in MATLAB/Simulink environment for a 1.5 kW induction machine. Table 2 shows the regroups the electrical and mechanical parameters values. Different simulation tests were carried out under the conditions, DC voltage E=150V; Reference stator flux $\phi_{s_{ref}} = 0.35Web$; $\Delta\phi_s = 0.01Web$, $\Delta\Gamma_e = 0.02N.m$; and the sampling time $T_s = 1e^4s$. The first test aims to evaluate the speed tracking efficiency. In fact, as shown in Figure 7, starting from a steady state of 600 rpm, 400 rpm acceleration and deceleration steps were applied respectively at t=1,2 s and t=3 s. We remark that the Anti-windup PI speed controller has achieved the test goals: no over/under-shoots, faster time response and better constancy in steady state. Figure 8 presents electromagnetic torque.

The stator currents Figure 9 and Figure 10 are sinusoidal and present less harmonics. The stator flux Figure 11 tracks its reference with good performance. The second test is to evaluate the disturbances rejection effectiveness. In fact, during this test, the speed was maintained at 600 rpm and a disturbance (80% of load torque (T_r)) was inserted at $t = 1.5s$ and removed at t=3s . As shown in Figure 12, the proposed PI Anti-windup controller has significant improvements; the rejection of load disturbances was done quickly. In addition, as schown in Figure 13, the developed torque follows the load torque. The compensations for disturbance are achieved by developed electromagnetic torque automatically.

Table 2. Induction machine parameters

Parameters	value
Rated Power P	1.5 kW
Voltage V	220/380 V
Number of Pair Poles n_p	2
Stator Resistance R_s	5.63 Ω
Rotor Resistance R_r	2.62 Ω
Stator Self-Inductance L_s	0.018 H
Rotor Self-Inductance L_r	0.018 H
Mutual Inductance M	0,20 H
Total inertia J	0,023 kg. m^2
Friction coefficient f	0,00155 N. m. s

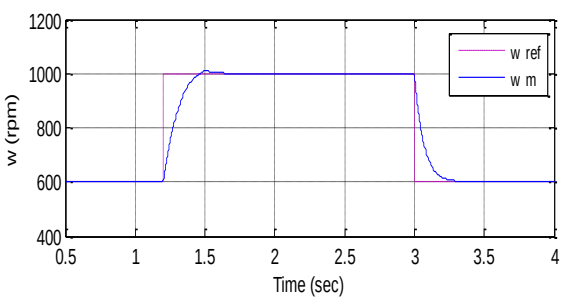

Figure 7. Speed tracking responses, case of 400 rpm acceleration/deceleration

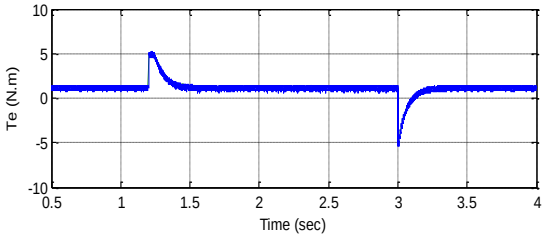

Figure 8. Electromagnetic Torque response

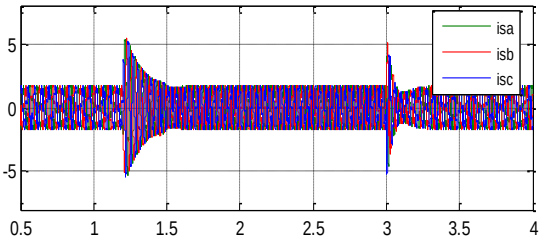

Figure 9. Stator current responses

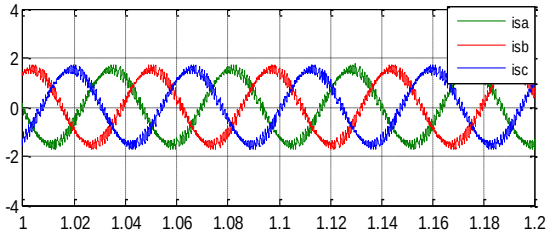

Figure 10. Zoom on stator current responses

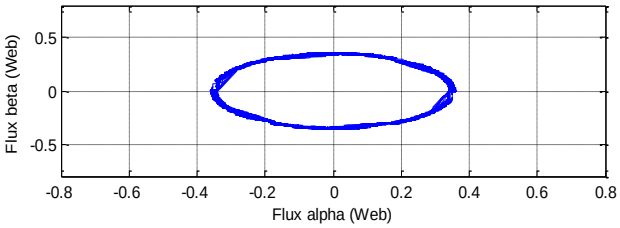

Figure 11. Stator flux in the αβ phase plane

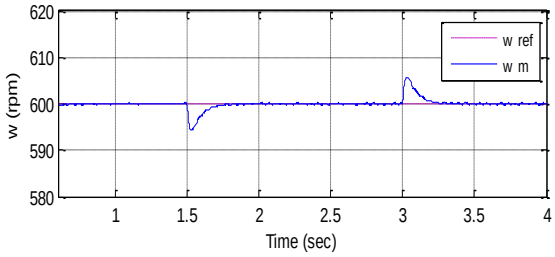

Figure 12. Disturbances rejection response for 80% of T_r and 600 rpm reference speed: speed response

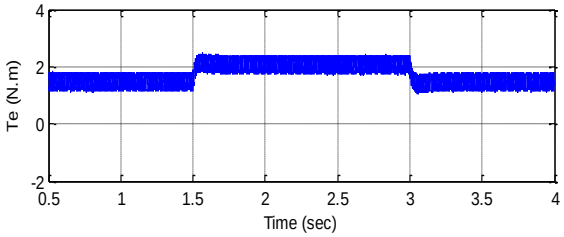

Figure 13. Disturbances rejection response for 80% of T_r and 600 rpm reference speed: torque response

6. EXPERIMENTAL SETUP AND PRACTICAL RESULTS

6.1. Experimental setup

The realized experimental setup is shown in Figure 14 and Figure 15. It consists of: (i) an IGBTs Voltage Inverter, (ii) the 1.5 KW induction motor (coupled in star) is driven under load with the help of DC generator mechanically coupled to the motor and having the following characteristics: 1KW, 220V, 6.5A, 2520rpm. The latter supplies a 4KW resistive bank to produce different load torques, (iii) A dSPACE 1104 board based on a 250 MHz 603-PowerPC- 64-bit processor and a slave-DSP based on a 20 MHz TMS320F240-16-bit microcontroller is used. The dSPACE works on Matlab/Simulink R2013b platform. dSPACE board is used with Control Desk software which makes the record of the results easy. It helps also by making the development of controllers effective and automates the experiments. With the dSPACE 1104 the user can design the drive in MATLAB/SimulinkR2013b and with the help of Real-Time Workshop (RTW) of MATLAB/Simulink R2013b and Real Time Interface (RTI), the user can convert them to real-time codes, (iv) A tachogenerator is used for speed sensor (15V for 1500rpm).

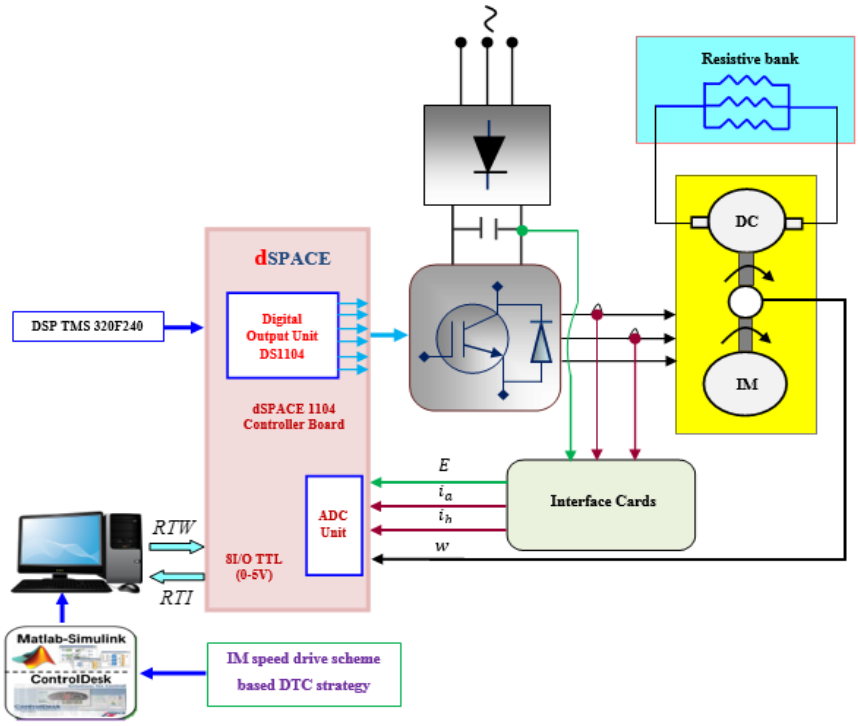

Figure 14. Experimental platform

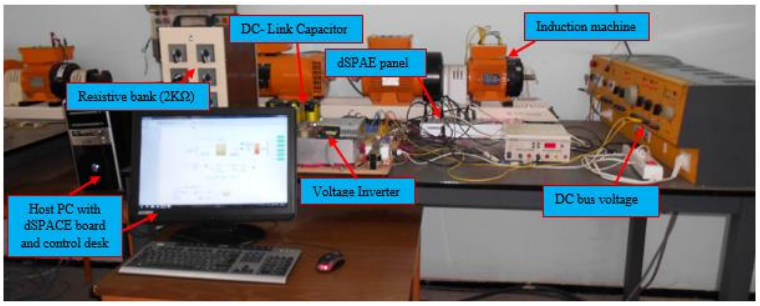

Figure 15. Different parts of experimental test bench and its dSPACE control

6.2. Practical results and discussion

To validate the simulation results, different practical tests were carried out under the conditions: DC voltage E=150V; Reference stator flux $\phi_{s_{ref}} = 0.35Web$; $\Delta\phi_s = 0.01Web$, $\Delta T_e = 0.02N.m$; and the sampling time $T_{ech} = 1e^{-4}s$. The first test aims to evaluate practically the speed tracking efficiency. In fact, as shown in Figure 16, starting from a steady state of 600 rpm, 400 rpm acceleration and deceleration steps were applied. We remark that the Anti-windup PI speed controller has achieved the test goals: no over/under-shoots, faster time response and better constancy in steady state. Figure 17 presents practical electromagnetic torque. Figure 18 and Figure 19 shows that the stator currents of the machine have a sinusoidal waveform and present less harmonics. The stator flux Figure 20 tracks its reference with good performance. the experimental results confirm the simulation results.

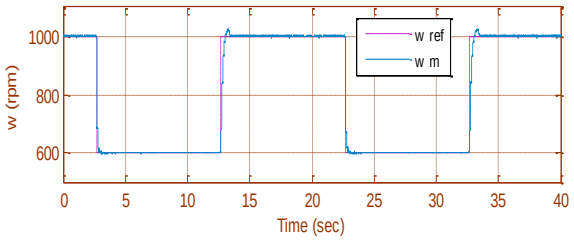

Figure 16. Practical speed tracking response, case of 400 rpm acceleration/deceleration

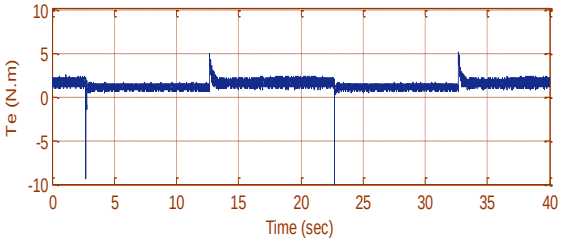

Figure 17. Practical electromagnetic torque response

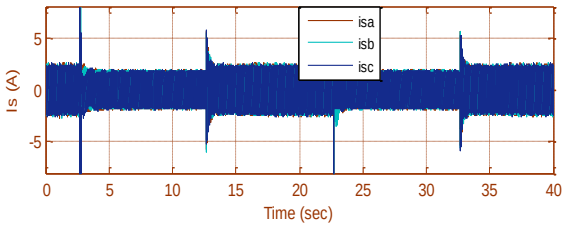

Figure 18. Practical stator currents responses

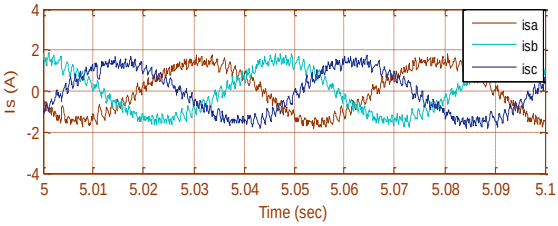

Figure 19. Zoom on stator currents responses

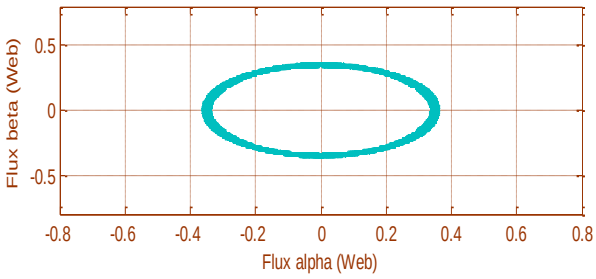

Figure 20. Practical stator flux in the αβ phase plane

The second test is to evaluate the disturbances rejection effectiveness. In fact, during this test, the speed was maintained at 600 rpm and a disturbance (80% of T_r) was inserted at $t = 13.4s$ and removed at t=20s. As shown in Figure 21, the proposed anti-windup PI controller offers significant improvements; load disturbance rejection was achieved quickly with the proposed controller. Moreover, as schown in Figure 22, the developed torque can follow the load torque. The compensations for disturbance are achieved by developed electromagnetic torque automatically. The experimental results confirm the simulation results.

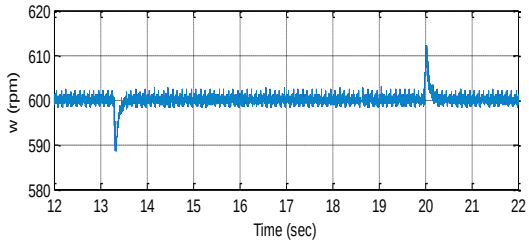

Figure 21. Experimental disturbances rejection response for 80% of T_r and 600 rpm reference speed: speed response

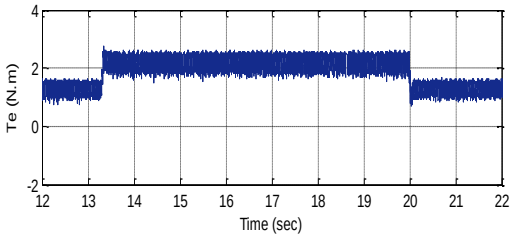

Figure 22. Experimental disturbances rejection response for 80% of T_r and 600 rpm reference speed: torque response

7. CONCLUSION

In this paper, we presented a simulation and real time implementation study of anti-windup PI controller in order to improve induction machine speed control based on direct torque control strategy. A model of proposed control scheme, based on the Matlab-Simulink simulation tool, has been proposed and validated through-out experimental test results. The experimental results show that the DTC method applied to an induction machine using an Anti-windup PI controller of speed present most interest and contribute to improvement the performance of system.

REFERENCES

[1] L. A. Brooks, E. L. Castro, J. L. Castro and C. U. Loo, "Flux-torque cross-coupling analysis of FOC schemes: Novel perturbation rejection characteristics," in *ISA Transactions*, vol. 58, pp. 446-461, September 2015, doi: 10.1016/j.isatra.2015.05.004.

[2] H. Chaikhy, M. Khafallah, A. Saad, K. Chikh and M. Es-saadi, "Assessment of direct torque control strategies for induction machine," *2012 International Conference on Multimedia Computing and Systems*, 2012, doi: 10.1109/ICMCS.2012.6320213.

[3] A. B. Jidin, N. R. B. N. Idris, A. H. B. M. Yatim, M. E. Elbuluk and T. Sutikno, "A wide-speed high torque capability utilizing overmodulation strategy in DTC of induction machines with constant switching frequency controller," in *IEEE Transactions on Power Electronics*, vol. 27, no. 5, pp. 2566-2575, May 2012, doi: 10.1109/TPEL.2011.2168240.

[4] P. K. Beher, M. K. Baher and A.K. Sahho, "Comparative analysis of scalar & vector control of induction motor through modeling & simulation," *International Journal of Innovative Research in Electrical, Electronics, Instrumentation and Control Engineering*, vol. 2, no. 4, pp. 1340-1344, 2014.

[5] S. Jacques, Z. Mokrani, S. Aissou, D. Rekioua and T. Rekioua, "Modeling and implementation of the direct torque control technique used in a relevant PV-powered pumping application," *Journal of Electrical Engineering (JEE)*, 2018. hal-02296862.

[6] L. Ouboubker, M. Khafallah, J. Lamterkati and K. Chikh, "Comparison between DTC using a two-level inverters and DTC using a three level inverters of induction motor," in *2014 International Conference on Multimedia Computing and Systems (ICMCS)*, 2014, pp. 1051-1058, doi: 10.1109/ICMCS.2014.6911167.

[7] H. Kawai, Y. Kouno and K. Matsuse, "Characteristics of speed sensorless vector control of parallel connected dual induction motor fed by a single inverter," in *Proceedings of the Power Conversion Conference-Osaka 2002 (Cat. No.02TH8579)*, 2002, pp. 522-527 vol.2, doi: 10.1109/PCC.2002.997571.

[8] G. Ramachandran, S. Veerana, S. Padmanaban, C. Sciences, "Vector control of a three-phase parallel connected two motor single inverter speed sensorless drive," *Turkish Journal of Electrical Engineering & Computer Sciences*, vol. 24, no. 5, pp. 4027-4041, 2016, doi: 10.3906/elk-1410-48.

[9] F. Yusivar, H. Haratsu, T. Kihara, S. Wakao and T. Onuki, "Performance comparison of the controller configurations for the sensorless IM drive using the modified speed adaptive observer," in *2000 Eighth International Conference on Power Electronics and Variable Speed Drives (IEE Conf. Publ. No. 475)*, 2000, pp. 194-200,
doi: 10.1049/cp:20000244.

[10] P. K. Nandam and P. C. Sen, "A comparative study of proportional-integral (PI) and integral-proportional (IP) controllers for dc motor drives," in *International Journal of Control*, vol. 44, no. 1, pp. 283-297, 2007, doi: 10.1080/00207178608933599.

[11] R. Hanus, M. Kinnaert and J. L. Henrotte, "Conditioning technique, a general anti-windup and bumpless transfer method," *Automatica*, vol. 23, no. 6, pp. 729-739, 1987, doi: 10.1016/0005-1098(87)90029-X.

[12] D. Zhang, H. Li and E. G. Collins, "Digital anti-windup PI controllers for variable-speed motor drives using FPGA and stochastic theory," *IEEE Transactions on Power Electronics*, vol. 21, no. 5, pp. 1496-1501, Sept. 2006, doi: 10.1109/TPEL.2006.882342.

[13] X. L. Li, J. G. Park and H. B. Shin, "Comparison and evaluation of anti-windup PI controllers," *Journal of Power Electronics*, vol. 11, no. 1, pp. 45-50, January 2011, doi: 10.6113/JPE.2011.11.1.045.

[14] J. Seok, "Frequency-spectrum-based antiwindup compensator for PI-controlled systems," in *IEEE Transactions on Industrial Electronics*, vol. 53, no. 6, pp. 1781-1790, Dec. 2006, doi: 10.1109/TIE.2006.885118.

[15] J. Seok, K. Kim and D. Lee, "Automatic mode switching of P/PI speed control for industry servo drives using online spectrum analysis of torque command," in *IEEE Transactions on Industrial Electronics*, vol. 54, no. 5, pp. 2642-2647, Oct. 2007, doi: 10.1109/TIE.2007.899824.

[16] N. J. Krikelis, "State feedback integral control with intelligent integrator," in *International Journal of Control*, vol. 32, no. 3, pp. 465-473, 1980, doi: 10.1080/00207178008922868.

[17] K. J. Åström and T. Hägglund, *PID controllers: Theory, design and tuning*, Research Triangle Park, NC: ISA, Jan. 1995.

[18] Hwi-Beon Shin, "New antiwindup PI controller for variable-speed motor drives," in *IEEE Transactions on Industrial Electronics*, vol. 45, no. 3, pp. 445-450, June 1998, doi: 10.1109/41.679002.

[19] K. Ohishi, E. Hayasaka, T. Nagano, M. Harakawa and T. Kanmachi, "High-performance speed servo system considering Voltage saturation of a vector-controlled induction motor," in *IEEE Transactions on Industrial Electronics*, vol. 53, no. 3, pp. 795-802, June 2006, doi: 10.1109/TIE.2006.874274.

[20] C. Bohn and D. P. Atherton, "An analysis package comparing PID anti-windup strategies," in *IEEE Control Systems Magazine*, vol. 15, no. 2, pp. 34-40, April 1995, doi: 10.1109/37.375281.
[21] A. Scottedward Hodel and C. E. Hall, "Variable-structure PID control to prevent integrator windup," in *IEEE Transactions on Industrial Electronics*, vol. 48, no. 2, pp. 442-451, April 2001, doi: 10.1109/41.915424.
[22] I. M. Chergui, M. Bourahla, "Application of the DTC control in the photovoltaic pumping system," *Energy Conversion and Management*, vol. 65, pp. 655-662, 2013, doi: 10.1016/j.enconman.2011.08.026.
[23] D. Rekioua, S. Bensmail, N. Bettar, "Development of hybrid photovoltaic-fuel cell system for stand-alone application," in *International Journal of Hydrogen Energy*, vol. 39, no. 3 pp. 1604-1611, 2014, doi: 10.1016/j.ijhydene.2013.03.040.
[24] S. Ziaeinejad, Y. Sangsefidi, H. Pairodin Nabi and A. Shoulaie, "Direct torque control of two-phase induction and synchronous motors," in *IEEE Transactions on Power Electronics*, vol. 28, no. 8, pp. 4041-4050, Aug. 2013, doi: 10.1109/TPEL.2012.2230409.
[25] T. Ouchbel, S. Zouggar, M.L. Elhafyani, M. Seddik, M. Oukili, A. Aziz and F.Z. Kadda, "Power maximization of an asynchronous wind turbine with a variable speed feeding a centrifugal pump," in *Energy Conversion and Management*, vol. 78, pp. 976-984, 2014, doi: 10.1016/j.enconman.2013.08.063.

BIOGRAPHIES OF AUTHORS

Lahcen Ouboubker was born in Morocco in 1983. He received the Master's degree in electrical engineering from the Faculty of Science Semlalia Marrakech, Morocco, in 2007 and the Ph.D degree in Electrical Engineering in 2017 from the National Higher School of Electricity and Mechanics (ENSEM), Hassan II University Casablanca, Morocco. Since July 2018, he has been with Ibn Zohr University, Morocco, where he is currently professor at the Faculty of Applied Sciences of Ait Melloul (FSAAM). His current research interests are advanced control for the AC Machines, renewable energy and advanced control of the power electronic converter.

Jawad Lamterkati was born in Morocco in 1981. He received the Master's degree in electrical engineering from the Faculty of Science Semlalia Marrakech, Morocco, in 2007 and the Ph.D degree in Electrical Engineering in 2017 from the National Higher School of Electricity and Mechanics (ENSEM), Hassan II University Casablanca, Morocco. Since June 2019, he has been with Higher School of Technology (ESTC), Hassan II University Casablanca, Morocco, where he is currently professor at the Electrical Engineering Department. His main fields of interest are modelling, control in power electronics, power converters (inverters, converters, controlled and uncontrolled rectifier) and motors drives.

Mohamed Khafallah was born in Morocco in 1964. He received B.Sc., M.Sc. and Doctorate degrees from Hassan II University, Casablanca, in 1989, 1991 and 1995 respectively, all in Electrical Engineering. In 1995 he joined the National High School of Electricity and Mechanics (ENSEM), Hassan II University, Casablanca, Morocco, where he is currently professor tutor in the Department Electrical Engineering and chief of Laboratory Energy and Electrical Systems (LESE). His main research interests the application of power electronics converts and motor drives. He has published a lot of research papers in international journals, conference proceedings as well as chapters of books.

Aziz El Afia received B.Sc., M. Sc. degrees from Hassan II University, Casablanca in 1990, 1994 respectively and the Ph.D. degree in Electrical Engineering from The National High School of Electrical and Mechanical Engineering (ENSEM), Hassan II University, Casablanca in 2009. Since 2011 he has been working as a Professor of Power Electronic at the National High School of Arts and Crafts of Casablanca (ENSAM). His current research interests are in power electronics converters and control of machines and drives for application from automotive to renewable energy.